

Experimental and Theoretical Characterization of the High-Affinity Cation-Binding Site of the Purple Membrane

Leonardo Pardo,* Francesc Sepulcre,[#] Josep Cladera,[#] Mireia Duñach,[#] Amílcar Labarta,[§] Javier Tejada,[§] and Esteve Padrós[#]

*Laboratori de Medicina Computacional, Unitat de Bioestadística, Facultat de Medicina, Universitat Autònoma de Barcelona, 08193 Bellaterra, Barcelona; [#]Unitat de Biofísica, Departament de Bioquímica i de Biologia Molecular, Facultat de Medicina, Universitat Autònoma de Barcelona, 08193 Bellaterra, Barcelona; and [§]Departament de Física Fonamental, Facultat de Física, Universitat de Barcelona, 08028 Barcelona, Spain

ABSTRACT Binding of Mn^{2+} or Mg^{2+} to the high-affinity site of the purple membrane from *Halobacterium salinarum* has been studied by superconducting quantum interference device magnetometry or by ab initio quantum mechanical calculations, respectively. The binding of Mn^{2+} cation, in a low-spin state, to the high-affinity site occurs through a major octahedral local symmetry character with a minor rhombic distortion and a coordination number of six. A molecular model of this binding site in the Schiff base vicinity is proposed. In this model, a Mg^{2+} cation interacts with one oxygen atom of the side chain of Asp⁸⁵, with both oxygen atoms of Asp²¹² and with three water molecules. One of these water molecules is hydrogen bonded to both the nitrogen of the protonated Schiff base and the Asp⁸⁵ oxygen. It could serve as a shuttle for the Schiff base proton to move to Asp⁸⁵ in the L-M transition.

INTRODUCTION

The purple membrane (PM) from *Halobacterium salinarum* is a specialized part of the cellular membrane that translocates protons under light absorption (Oesterhelt and Stoerkenius, 1973). It contains a unique transmembrane protein, bacteriorhodopsin (BR), which is formed of an apoprotein of M_r 26,000 and a retinal molecule bound to the protein through a protonated Schiff base. Native purple membrane (λ_{max} 568 nm, light adapted) contains five bound cations (one Ca^{2+} and four Mg^{2+}) per bacteriorhodopsin molecule (Kimura et al., 1984; Chang et al., 1985). Acidification of a PM suspension gives rise to a blue form absorbing at ~ 600 nm, which is due to the protonation of Asp⁸⁵, the Schiff base counterion (Subramaniam et al., 1990; Jonas and Ebrey, 1991; Metz et al., 1992). Upon deionization, the apparent pK of the purple to blue transition in water suspension increases by ~ 2.5 pH units, as compared to the native membrane. The deionized membrane can be fully regenerated by adding a wide variety of cations (Kimura et al., 1984; Chang et al., 1985; Ariki and Lanyi, 1986). The blue membrane has an altered photocycle, and it is unable to translocate protons (Mowery et al., 1979; Chang et al., 1985). On the other hand, a relationship between the retinal pocket and some of the divalent cation-binding sites has been shown (Duñach et al., 1986; Sepulcre and Padrós, 1992).

The binding of the Mn^{2+} cations to the blue membrane at pH 5 was determined, by spin-labeling methods, to consist

of a high-affinity site (affinity constant $26 \mu\text{M}^{-1}$), three sites of $2 \mu\text{M}^{-1}$, and one site of $0.6 \mu\text{M}^{-1}$ (Duñach et al., 1987). Similar values were found at pH 5 for Ca^{2+} binding, with a rapid-filtration technique (Duñach et al., 1988b). Other workers reported, by using potentiometric techniques, the presence of only two medium-affinity sites ($2.4 \mu\text{M}^{-1}$ and $0.4 \mu\text{M}^{-1}$, respectively) plus four low-affinity sites at pH 4.3 (Zhang et al., 1992). In addition, extended x-ray absorption fine structure (EXAFS) studies provided evidence for a tetragonal coordination of Mn^{2+} with six oxygen atoms located in the protein molecule (Sepulcre et al., 1996).

The magnetic susceptibility technique provides an independent means of corroborating our previous EXAFS results (Sepulcre et al., 1996). In the present work, we collected magnetic susceptibility data obtained by superconducting quantum interference device (SQUID) magnetometry from the blue membrane substituted with one Mn^{2+} cation occupying the high-affinity site. In the scope of the crystal field theory, this study allows us to deduce both the local symmetry and the electronic structure of Mn^{2+} bound to this site. A possible structure for the high-affinity cation-binding site in bacteriorhodopsin is proposed; its feasibility is tested by quantum mechanical calculations.

MATERIALS AND METHODS

Membrane preparation

The purple membrane was isolated from the *Halobacterium salinarum* strain S9 as described in Oesterhelt and Stoerkenius (1974). Deionized samples were prepared by passing membrane suspensions through a cation exchange column (Dowex 50W). After addition of enough MnCl_2 to fill the high-affinity site (Duñach et al., 1987), the pH of the sample was adjusted to pH 5 with small amounts of concentrated NaOH. Correct binding of cations was controlled by observing the blue shift of the visible absorption spectrum (Duñach et al., 1987). Five milligrams of the partially regenerated membrane was lyophilized for magnetic susceptibility measurements.

Received for publication 28 July 1997 and in final form 27 April 1998.

Address reprint requests to Dr. Esteve Padrós, Unitat de Biofísica, Departament de Bioquímica i de Biologia Molecular, Facultat de Medicina, Universitat Autònoma de Barcelona, 08193 Bellaterra, Barcelona, Spain. Tel.: 34-3-581-1870; Fax: 34-3-581-1907; E-mail: epadros@cc.uab.es.

© 1998 by the Biophysical Society

0006-3495/98/08/777/08 \$2.00

SQUID magnetometry

Magnetic susceptibility measurements were carried out by using a SQUID magnetometer working in a temperature range between 2 K and 310 K, and with an applied magnetic field, H , of 5 kOe. Experimental error of temperature measurements were less than 0.1 K, whereas the estimated error for each $\chi(T)$ point was below 5%. The diamagnetic correction, due to both the cylindrical plastic boat and the membrane, was achieved by recording the thermal dependence of the susceptibility under different values of the applied magnetic field ranging from 2 kOe to 15 kOe.

Near room temperature, the temperature dependence of the susceptibility can be expressed as

$$\chi(T) = \frac{C}{T} + \chi_d$$

where C is the Curie constant and χ_d is the diamagnetic susceptibility due to the container and membrane diamagnetic atoms. Therefore, $\chi(T) \cdot T = C + \chi_d \cdot T$, and $\chi(T) \cdot T$ has a linear dependence on T , where χ_d is the corresponding slope. We verified this linearity with different values of H , and by using the preceding equation, we evaluated the average χ_d value.

Susceptibility calculations

The energetically lowest lying multielectron terms of the Mn^{2+} cation have been obtained, in the scope of a single-point crystal-field model, from the diagonalization of the Hamiltonian,

$$H_0 = H_{ee} + H_{cf}$$

on the basis of the $3d^5$ configuration. In this Hamiltonian, H_{ee} corresponds to the Coulomb repulsion between electrons, and H_{cf} accounts for the crystal field potential, which for the position of the Mn^{2+} cations in the purple membrane is assumed to have C_{2v} symmetry (tetragonal with rhombic distortion) and can be expanded in terms of the V_{em} operators and the electronic splittings ϵ_i and D , of the $3d^1$ energy levels (Eicher and Trautwein, 1969; see Fig. 1). For realistic values of the crystal field parameters, the low lying multielectron wave functions are 4E , 2B_2 , 2E , 4A_2 , and 6A_1 (Thomanek, 1975). In this subset of eigenfunctions, the total Hamiltonian H

$$H = H_0 + H_{so} + H_m$$

is rediagonalized, where H_{so} represents the spin-orbit coupling and H_m stands for the interaction with the externally applied magnetic field. The resulting term scheme is used to calculate the thermal dependence of the magnetic susceptibility (Alabart et al., 1990).

Geometries and energetics

All of the quantum mechanical calculations were performed by ab initio methods in the GAUSSIAN-94 system of programs (Frisch et al., 1995).

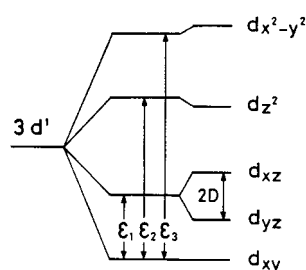


FIGURE 1 Splitting of $3d^1$ levels in C_{4v} and C_{2v} symmetry environments.

The structure optimizations of $(\text{Mg}^{2+} \cdot 2\text{H}_2\text{O})$, $(\text{Mg}^{2+} \cdot 3\text{H}_2\text{O})$, and Mg^{2+} complexes were performed with the 3-21G* basis set. Energy calculations of the interaction between the cation and the protein model, E_{int} , were performed with the 6-31 + G* basis set at the level of Restricted Hartree-Fock (RHF). Solvation energies, E_{solv} , of isolated $(\text{Mg}^{2+} \cdot 2\text{H}_2\text{O})$ and $(\text{Mg}^{2+} \cdot 3\text{H}_2\text{O})$ were calculated with a polarized continuum model (Miertus et al., 1981; Miertus and Tomasi, 1982), as implemented in GAUSSIAN-94. The enthalpy of formation of the complex between the cation and the protein model was calculated as $\Delta H_f = E_{\text{int}} - E_{\text{solv}}$.

The model of BR sites employed in the calculation of E_{int} comprised the C_α and the side chains of Asp⁸⁵, Asp²¹², and Lys²¹⁶ Schiff base. The retinal chromophore bound to Lys²¹⁶ via a protonated Schiff base was replaced with a $=\text{CH}_2$ group. During the energy optimization of the system, the position of the atoms C_α of Asp⁸⁵ and Asp²¹², and C_α , C_β , C_γ , C_δ , C_ϵ , N_ϵ , and C_{15} of Lys²¹⁶ Schiff base were kept fixed at the positions originally determined by electron microscopy (Henderson et al., 1990).

RESULTS

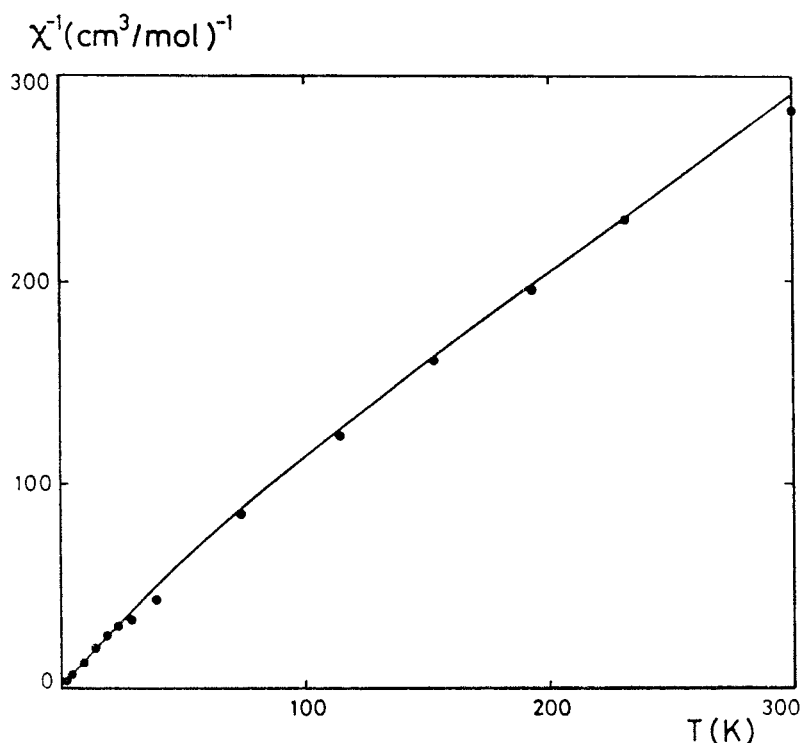
Magnetic susceptibility experiments

The results of the magnetic susceptibility measurements are given in Fig. 2. These data have been fitted to the theoretically calculated magnetic susceptibility, using as adjustable parameters the values of the $3d^1$ splittings, ϵ_i ($i = 1, 2, 3$) and D , and the spin-orbit coupling constant λ , which can be expressed as a function of the free ion spin-orbit coupling constant $\lambda_0 = 300 \text{ cm}^{-1}$ and a fit parameter taking into account the covalency degree of the binding of the Mn^{2+} cations with its ligands ($\lambda = \lambda_0 \alpha^2$). Table 1 summarizes the results of the fitting procedure, compared with the experimental data. The resulting energy diagram of the low-lying multielectron states of Mn^{2+} cation is shown in Fig. 3.

The values obtained for the crystal-field parameters ϵ_i and D can be correlated with the local structure of the Mn^{2+} site. The ϵ_3 value gives the energy of the antibonding single electron orbital $d_{x^2-y^2}$ referred to the d_{xy} orbital. The high value found for ϵ_3 suits well the major tetragonal character of the local symmetry around the Mn^{2+} location site. This suggests a strong interaction between the Mn^{2+} ion and the ligands lying in the xy plane. ϵ_2 is the energy of the antibonding $3d_{z^2}$ orbital referred to the $3d_{xy}$. This value is much lower than ϵ_3 (see Table 1). This indicates that the interaction between the Mn^{2+} and the ligands lying in the z direction is different between them or is different from the other ligands of the xy plane. In addition, the low value obtained for the D parameter indicates a minor rhombic local distortion around the Mn^{2+} site in the xy plane.

Comparison of our results with those previously published for heme systems and Mn^{2+} -phthalocyanine complexes (Thomanek et al., 1977; Labarta et al., 1984, 1985) show that the 2E low-spin state appears as the ground term only in the present case. This is a consequence of a higher value of the crystal field intensity as it is characterized by the ϵ_3 parameter. Therefore, it is reasonable to assume that the interactions between the Mn^{2+} cation and the ligands, indicated by e_i/r_i ratios (where e_i is the effective neighbor charge and r_i is the distance between this neighbor charge and the cation) are higher in our case than in the heme systems or in the Mn^{2+} -phthalocyanine complex.

FIGURE 2 Plot of P^{-1} values as a function of temperature. The continuous line corresponds to the least-squares fit of P^{-1} to the experimental values, using as adjustable parameters the values of the $3d^1$ splittings and D , and the spin-orbit coupling constant 8.



It should be highlighted that these results are in good agreement with EXAFS data, which demonstrated that Mn^{2+} in the high-affinity binding site presents a distorted tetrahedral symmetry with a coordination number of 6. A location of this site within the protein and not in the lipid phase was also suggested (Sepulcre et al., 1996). The independence of the two techniques used reinforces the conclusions obtained. Thus, having corroborated the metal coordination and geometry, we proceeded toward finding a suitable molecular environment for the cation.

TABLE 1 Least-squares parameters obtained from the χ_m^{-1} fitting procedure, and calculated values of the energy of several multielectron terms corresponding to the $3d^5$ configuration

ϵ_1	500 cm^{-1} (arbitrarily fixed)
ϵ_2	16527 ± 200 cm^{-1}
ϵ_3	35705 ± 500 cm^{-1}
D	-30 ± 20 cm^{-1}
α^2	0.70 ± 0.05
Curie constant	1.02 $emu \cdot K \cdot mol^{-1}$ (experimental value, 1.07)*
Curie temperature	8.5 K (experimental value, 8.7)*
Magnetic moment	2.86 Bohr's magneton (experimental value, 2.93)*
2E	0 cm^{-1}
4A_2	505 ± 50 cm^{-1}
2B_2	1096 ± 100 cm^{-1}
4E	≥ 5800 cm^{-1}
6A_1	≥ 7000 cm^{-1}
Gyromagnetic constants:	$g_x = 0.977$
	$g_y = 0.209$
	$g_z = -1.551$

*Experimental values correspond to the fit of the $\chi_m^{-1}(T)$ points to the Curie-Weiss law.

In the following, we take as equivalent a binding site occupied indistinctly by Ca^{2+} , Mn^{2+} , or Mg^{2+} .

Several previous results can aid in defining a probable location for the cation-binding site. Although indirect effects could also account for the observed events, it is generally thought that a cation site near the retinal Schiff base is necessary to explain 1) the well-known effect of cation

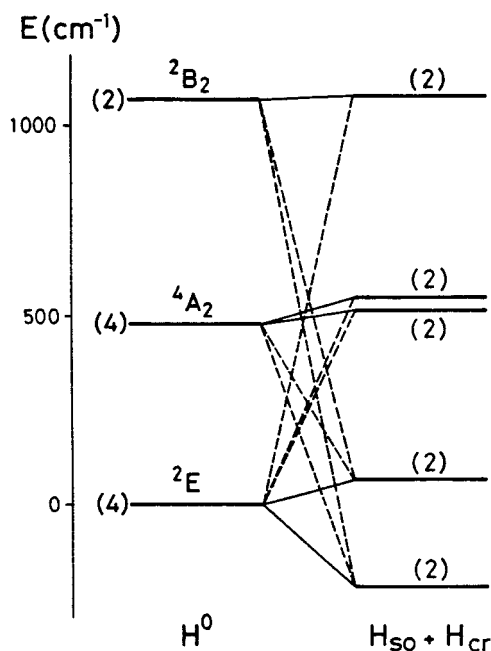


FIGURE 3 Electronic structure levels of Mn^{2+} occupying the high-affinity site of purple membrane.

binding on the visible absorption maximum; 2) the change in number and affinities of the cation-binding sites by retinal removal (Chang et al., 1986; Duñach et al., 1986; Zhang et al., 1992); and 3) the change in cation binding by Schiff base reduction or by isomerization to 9-*cis*, i.e., the pink membrane (Duñach et al., 1988a). If the retinal absorption maximum is modulated primarily by the protonation state of Asp⁸⁵ and its distance to the Schiff base, a natural site for the cation would be near Asp⁸⁵. In addition, experiments with mutated BR demonstrated a strong influence of Asp⁸⁵ and Asp²¹², especially the latter, on the binding affinity of Ca²⁺ (Zhang et al., 1993). On the other hand, EXAFS results indicated a maximum of three carbon atoms forming the second shell of the Mn²⁺ cation and excluded a participation of P or S atoms (Sepulcre et al., 1996).

Taking into account the above considerations, and the arrangement of the lateral chains near the Schiff base that arise from the structural model of Henderson et al. (1990), we have undertaken a theoretical analysis of the possible environment of a Mg²⁺ cation near the Schiff base.

A model of the binding site in the Schiff base environment

As a working hypothesis, we can assume that Mg²⁺ binds to BR through an octahedral coordination shell formed by the two carboxylic side chains of Asp⁸⁵ and Asp²¹², located in the base of the pyramid, and two discrete water molecules located in the axis. To evaluate computationally the feasibility of this hypothesis, a molecular model consisting of (Mg²⁺ · 2H₂O) and the side chains of Asp⁸⁵, Asp²¹², and the Schiff base was energy optimized. During the optimization (see Fig. 4 *A* and Materials and Methods), the C_α of the amino acids and the heavy atoms of the side chain of Lys²¹⁶ forming the Schiff base were kept fixed at the positions originally determined by electron microscopy (Henderson et al., 1990). For a buried cation in the interior regions of BR, it is clear that the cation must be desolvated. We considered first the contribution of solvation energies to the stabilization of the proposed complex. Results in Table 2 show the obtained values of E_{int} , E_{solv} and ΔH_f . As expected, E_{solv} is very high: -330.0 kcal/mol for (Mg²⁺ · 2H₂O). This energy is compensated for by the strong interaction with the highly polar sites on the protein model: -403.1 kcal/mol, resulting in a value of ΔH_f of -73.1 kcal/mol. The negative sign in ΔH_f indicates that the formation of the complex is favorable. It is important to clarify that the calculation of ΔH_f does not include the change in solvation energy of BR or its conformational change. However, given the large value of ΔH_f obtained in the formation of the complex, inclusion of these terms into ΔH_f is expected not to modify the obtained preference of the complex over the isolated ligands.

We can conclude that the binding of the divalent cation to the retinal pocket of BR, through the side chains of Asp⁸⁵

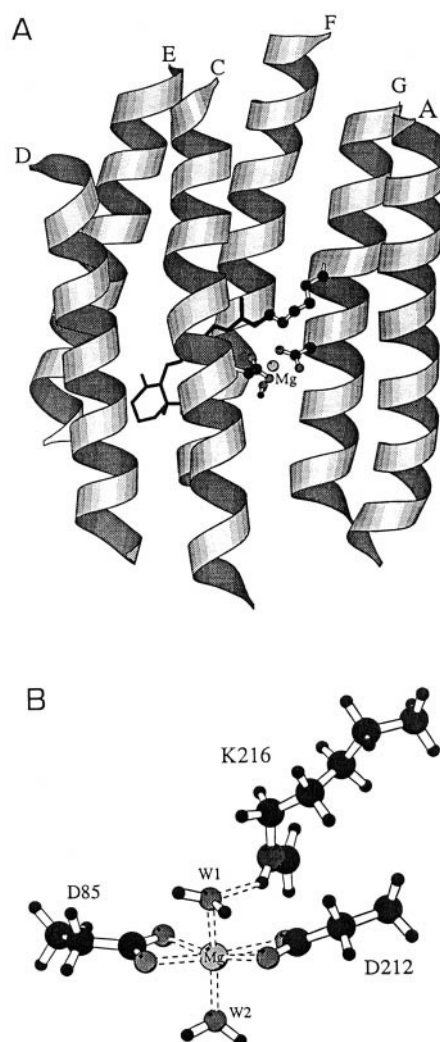


FIGURE 4 A model of the cation-binding site of bacteriorhodopsin. (*A*) Ribbon representation of the BR helical segments, including all-*trans* retinal, the Mg²⁺ cation, and part of the side chains of D85 and D212. Helix B was omitted for clarity. (*B*) Detailed view of the Mg²⁺-binding site, including two water molecules, W1 and W2. The atomic coordinates were taken from the work of Henderson et al. (1990). Figure was created using MOLSCRIPT (Kraulis, 1991).

and Asp²¹², is energetically feasible despite the presence of the positive charge of the Schiff base. Fig. 4 *B* presents a detailed view of the computed cation-binding site. Selected geometrical parameters of the optimized structure are shown in Table 3. The proposed interaction between the cation and the Asp residues is directly satisfied by the geometry constructed here. As can be seen in Fig. 4 *B* and Table 3, the Mg²⁺ cation has an octahedral coordination shell formed in the base of the pyramid by the O_δ atoms of Asp⁸⁵ (Mg²⁺...O_δ distances of 2.08 and 2.23 Å), and the O_δ atoms of Asp²¹² (Mg²⁺...O_δ distances of 2.23 and 2.36 Å); and at the vertex of the pyramid by two water molecules (W1 and W2; Mg²⁺...O_w distances of 2.11 and 1.96 Å, respectively). The mean interatomic distance between Mg²⁺ and O, obtained with *ab initio* structure optimization,

TABLE 2 Energy of interaction, energy of solvation, and enthalpy of formation of the complex between the cation and the protein model

Cation	E_{solv}	Protein	E_{int}	ΔH_f
(Mg ²⁺ · 2H ₂ O)	−330.0	Asp ⁸⁵ · Asp ²¹² · Lys ²¹⁶	−403.1	−73.1
Mg ²⁺		Asp ⁸⁵	−367.5	
Mg ²⁺		Asp ²¹²	−351.1	
(Mg ²⁺ · 3H ₂ O)	−292.1	Asp ⁸⁵ · Asp ²¹² · Lys ²¹⁶	−351.9	−60.8
Mg ²⁺		Asp ⁸⁵	−317.0	
Mg ²⁺		Asp ²¹²	−362.6	

E_{int} , Energy of interaction; E_{solv} , energy of solvation; ΔH_f , enthalpy of formation. Values are in kcal/mol.

is in very good agreement with the experimental distance between Mn²⁺ and O, obtained with the EXAFS technique (Sepulcre et al., 1996; 2.16 versus 2.17 Å; see Table 3). In addition, the water molecule located in the upper vertex of the pyramid is hydrogen bonded to the protonated Schiff base nitrogen.

However, these results are not in good agreement with some experimental determinations. In particular, mutation of Asp⁸⁵ to Asn decreases the affinity of BR for Ca²⁺ by about three times, whereas mutation of Asp²¹² to Asn decreases the affinity by 15 times (Zhang et al., 1993). This suggests that the cation is more tightly bound to Asp²¹² than to Asp⁸⁵. The values of E_{int} obtained for the interaction between Mg²⁺ and both Asp residues, shown in Table 2, are not in agreement with this rank order of affinities. Thus the model structure depicted in Fig. 4 B cannot explain the different observed affinities of Asp⁸⁵ and Asp²¹² for the cation.

A possibility for decreasing the energy of interaction of Mg²⁺ with Asp⁸⁵ is the introduction of a new water molecule in the *xy* plane. The optimized geometry of the system is shown in Fig. 5. The Mg²⁺ cation has the O_δ atoms of Asp²¹² (Mg²⁺ ··· O_δ distances of 2.24 and 2.09 Å), the O_{δ1} atom of Asp⁸⁵ (Mg²⁺ ··· O_{δ1} distance of 2.18 Å), and the oxygen atom of a water (W3) molecule (Mg²⁺ ··· O_w distance of 2.02 Å), as equatorial ligands. The axis of the

pyramid is formed by the other two water molecules (Mg²⁺ ··· O_w distances of 2.20 and 1.99 Å). The average interatomic distance between Mn²⁺ and O is 2.12 Å (Table 3). In addition to the above interactions the system contains hydrogen bonds between the O_{δ2} atom of Asp⁸⁵ and W2 and W3 (see Fig. 5 and Table 3). It is quite evident from the value of ΔH_f in Table 2 that the binding of Mg²⁺ · 3H₂O to BR (Asp⁸⁵ · Asp²¹² · Lys²¹⁶ Schiff base) remains favorable (−60.8 kcal/mol). Furthermore, the different coordination of Mg²⁺ in this model relative to the previous one shown in Fig. 4 B results in a predicted order of affinities between Mg²⁺ and Asp⁸⁵ and Asp²¹², based on the energies of the interaction (see Table 2), that qualitatively reproduces the rank order of affinities found experimentally. It also agrees with having a maximum of 3 C atoms in the second coordination shell, as deduced from the EXAFS results (Sepulcre et al., 1996).

DISCUSSION

The obtained molecular model of the high-affinity cation-binding site of BR suggests that the Mg²⁺ cation can be positioned between Asp⁸⁵, Asp²¹², the protonated Schiff base, and three water molecules. This model reproduces the octahedral coordination shell determined in the magnetic

TABLE 3 Selected distances of the optimized molecular models consisting of (Mg²⁺ · 2H₂O) or (Mg²⁺ · 3H₂O) and the side chains of Asp⁸⁵, Asp²¹², and Lys²¹⁶ of BR

Residue (atom)	Asp ⁸⁵		Asp ²¹²		W1	W2	W3	Mean	Exp
	O _{δ1}	O _{δ2}	O _{δ1}	O _{δ2}	O _w	O _w	O _w		
(Mg ²⁺ · 2H ₂ O) ··· Asp ⁸⁵ · Asp ²¹² · Lys ²¹⁶									
Mg ²⁺	2.08	2.23	2.23	2.36	2.11	1.96		2.16	
Lys ²¹⁶ (N _ε)					2.88				
Lys ²¹⁶ (H _ε)					2.05				
(Mg ²⁺ · 3H ₂ O) ··· Asp ⁸⁵ · Asp ²¹² · Lys ²¹⁶									
Mg ²⁺	2.18		2.24	2.09	2.20	1.99	2.02	2.12	
Lys ²¹⁶ (N _ε)					2.68				
Lys ²¹⁶ (H _ε)					1.79				
W1 (O _w)	2.41								
W1 (H _w)	1.60								
Asp ⁸⁵ (O _{δ2})						2.77	2.63		
(Mn ²⁺) ··· BR									2.17

Distances are in Å.

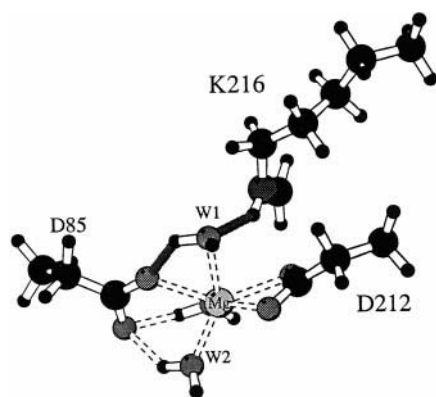


FIGURE 5 Optimized geometry of the cation-binding site of bacteriorhodopsin. The Mg^{2+} cation has the O δ atoms of Asp²¹², the O δ 1 atom of Asp⁸⁵, and the oxygen atom of a water molecule (not labeled, located behind the Mg^{2+} cation) as equatorial ligands. The axis of the pyramid is formed by the other two water molecules (W1 and W2).

susceptibility experiments, the distance between Mn²⁺ and O obtained with the EXAFS technique (Sepulcre et al., 1996), and the rank order of affinities between the cation, Asp⁸⁵, and Asp²¹² determined by site-directed mutagenesis (Zhang et al., 1993). In addition, difference infrared spectroscopy experiments (Fischer et al., 1994) have detected the presence of a water molecule, located in the active site of BR, which is structurally active during the BR6K primary phototransition. The same authors postulated the possibility that this structurally active water molecule was located between Asp⁸⁵ and the protonated Schiff base. The most salient geometrical feature of the model proposed here (Fig. 5) is the presence of a water molecule (W1) hydrogen bonded to both the O δ 1 atom of Asp⁸⁵ and the N ζ atom of the Lys²¹⁶ Schiff base, at distances of 2.41 and 2.68 Å, respectively (see Table 3 and *solid lines* in Fig. 5). The role of this water molecule might be to act as a shuttle for the H^+ between N ζ (Lys²¹⁶ Schiff base) and O δ (Asp⁸⁵) at the level of the M412 intermediate. The protonation of Asp⁸⁵ would obviously break its interaction with Mg^{2+} , increasing the interaction $Mg^{2+} \cdots Asp^{212}$ and severely perturbing the water structure, thus decreasing the interactions between helices C and G. In this respect, our model agrees with the movements of helix G in the M412 intermediate that have been described by diffraction techniques (Subramaniam et al., 1993; Kamikubo et al., 1996).

The recent 2.5-Å x-ray structure of BR (Pebay-Peyroula et al., 1997) has identified eight water molecules in the proton pathway. However, none of these molecules were within hydrogen-bonding distance of Asp⁸⁵. Notably, their experimentally determined distance of 4.1 Å between the O δ atom of Asp⁸⁵ and the N ζ atom of the Lys²¹⁶ Schiff base is in very good agreement with the value of 4.24 Å obtained in the present molecular model. On the other hand, the high-resolution electron diffraction BR structure of Kimura et al. (1997) gives further support for the ionized state of both Asp⁸⁵ and Asp²¹². This raises the question of how the retinal

Schiff base remains protonated within the membrane in the presence of these two negatively charged residues. The location of a cation in the neighboring Schiff base can give some clue to this issue. Thus the positioning of Mg^{2+} in the retinal pocket neutralizes these two negative charges, favoring the protonated state of the retinal Schiff base. In the M412 intermediate, the resulting isomerization of the retinal to 13-*cis* and the accompanying conformational changes might decrease the interaction between Mg^{2+} and Asp⁸⁵, facilitating its protonation from the Schiff base.

One of the interesting aspects of the current BR models is the location and orientation of the Arg⁸² side chain. Whereas the structural studies place the side chain of Arg⁸² at a distance from Asp⁸⁵ or Asp²¹² where it is unable to form ionic interactions (Henderson et al., 1990; Grigorieff et al., 1996; Pebay-Peyroula et al., 1997; Kimura et al., 1997), other studies place Arg⁸² close to Asp⁸⁵ (Logunov et al., 1995; Scharnagl et al., 1995). In the absence of a cation, this last prediction is likely, because there would be a clear tendency to neutralize the two negative charges of the aspartic side chains. We have explored the possibility that Asp⁸⁵ could achieve interaction with both the Mg^{2+} cation and the polar headgroup of Arg⁸² through the O δ atoms. The optimization of this system produced a situation in which the side chain of Arg⁸² was pointing toward the opposite direction of the retinal pocket and thus was far from the carboxylic headgroups of the Asp residues (results not shown). We can conclude, from this simulation, that Arg⁸² cannot form part of the retinal-binding pocket if the divalent cation is bound to the side chains of Asp⁸⁵ and Asp²¹².

A model similar to that of Fig. 5 has been proposed by Birge and co-workers, on the basis of two-photon and microwave spectroscopies (Stuart et al., 1995; Birge et al., 1996). Whereas the two models share an analogous disposition of side chains around the cation, we feel that our model conforms more closely to the requirements of our calculations plus mutagenic and EXAFS results. For example, the Ca²⁺ is directly ligated only to Asp⁸⁵ in figures 1a and 8a of Birge et al. (1996) and indirectly through water molecules to Asp²¹², a situation that will not conform to the reported affinities for these two carboxylic residues. Furthermore, in this case the energy of interaction will probably not be sufficient to surpass the energy of solvation of the Ca²⁺ cation.

Recently Roselli et al. (1996) studied the binding of Yb³⁺ in both bacteriorhodopsin and regenerated BR. They found an identical binding site for bacteriorhodopsin and BR, involving phospholipid headgroups, and carboxylic and tyrosine side chains. Thus this site must lie at or near the surface, a location clearly different from the site postulated in the present work. This difference in location may be due to the higher binding affinity of lanthanides for the PO₂⁻ headgroups, as compared to Ca²⁺ or Mg^{2+} (Roselli et al., 1996).

Fu et al. (1997) have recently suggested that the retinal pocket cannot contain the color-controlling cation binding site. This conclusion was based on the induction of the blue-to-purple transition by large sized cations (also docu-

mented in Tan et al., 1996), which can only occupy a surface location. However, taking into account the suggested existence of several proton channels through which Asp⁸⁵ can be protonated (Friedman et al., 1997), it is likely that cation binding can affect the state of protonation of Asp⁸⁵ (and thus the purple-to-blue transition) in different ways: 1) by binding in the neighboring Schiff base; 2) by influencing the proton channels' conductivity through changes in protein conformation or through changes in the pK_a of key side chains; 3) by changing the proton concentration at the entrance of the channel or even at the membrane surface. The fact that it is possible to obtain the purple form of the deionized membrane by increasing the pH (pK_a of ~5.4; Duñach et al., 1988a) gives support to the latter effect.

This work was supported in part by DGICYT grants to LP (PB95-0624) and EP (PB95-0609), a DGR grant to EP (1995SGR00481), and a Fundació La Marató TV3 grant to LP (14/97). Computations were performed at the Centre de Computació i Comunicacions de Catalunya.

REFERENCES

- Alabart, J. R., V. Moreno, A. Labarta, J. Tejada, and E. Molins. 1990. Electronic structure determination and dynamical properties of iron(II)-guanosine-5'-monophosphate complex via Mossbauer and magnetic susceptibility measurements. *J. Chem. Phys.* 92:6131–6139.
- Ariki, M., and J. K. Lanyi. 1986. Characterization of metal ion-binding sites in bacteriorhodopsin. *J. Biol. Chem.* 261:8167–8174.
- Birge, R. R., D. S. K. Govender, K. C. Izgi, and E. H. L. Tan. 1996. Role of calcium in the proton pump of bacteriorhodopsin. Microwave evidence for a cation-gated mechanism. *J. Phys. Chem.* 100:9990–10004.
- Chang, C.-H., J. G. Chen, R. Govindjee, and T. G. Ebrey. 1985. Cation binding by bacteriorhodopsin. *Proc. Natl. Acad. Sci. USA.* 82:396–400.
- Chang, C.-H., R. Jonas, S. Melchior, R. Govindjee, and T. G. Ebrey. 1986. Mechanism and role of divalent cation binding of bacteriorhodopsin. *Biophys. J.* 49:731–739.
- Cladera, J., M. L. Galisteo, M. Sabés, P. L. Mateo, and E. Padrós. 1992a. The role of retinal in the thermal stability of the purple membrane. *Eur. J. Biochem.* 207:581–585.
- Cladera, J., M. Sabés, and E. Padrós. 1992b. Fourier transform infrared analysis of bacteriorhodopsin secondary structure. *Biochemistry.* 31:12363–12368.
- Duñach, M., E. Padrós, A. Muga, and J. L. Arrondo. 1989. Fourier-transform infrared studies on cation binding to native and modified purple membranes. *Biochemistry.* 28:8940–8945.
- Duñach, M., E. Padrós, M. Seigneuret, and J. L. Rigaud. 1988a. On the molecular mechanism of the blue to purple transition of bacteriorhodopsin. *J. Biol. Chem.* 263:7555–7559.
- Duñach, M., M. Seigneuret, J. L. Rigaud, and E. Padrós. 1986. The relationship between the chromophore moiety and the cation binding sites in bacteriorhodopsin. *Biosci. Rep.* 6:961–966.
- Duñach, M., M. Seigneuret, J. L. Rigaud, and E. Padrós. 1987. Characterization of the cation binding sites of the purple membrane. Electron spin resonance and flash photolysis studies. *Biochemistry.* 26:1179–1186.
- Duñach, M., M. Seigneuret, J. L. Rigaud, and E. Padrós. 1988b. Influence of cations on the blue to purple transition of bacteriorhodopsin. *J. Biol. Chem.* 263:17378–17384.
- Ebrey, T. G. 1993. Light energy transduction in bacteriorhodopsin. In *Thermodynamics of Membrane Receptors and Channels*. M. Jackson, editor. CRC Press, Boca Raton, FL. 353–387.
- Eicher, H., and A. Trautwein. 1969. Electronic structure quadrupole splittings of ferrous iron in haemoglobin. *J. Chem. Phys.* 50:2540–2551.
- Fischer, W. B., S. Sonar, T. Marti, H. G. Khorana, and K. J. Rothschild. 1994. Detection of a water molecule in the active-site of bacteriorhodopsin: hydrogen bonding changes during the primary photoreaction. *Biochemistry.* 33:12757–12762.
- Friedman, N., I. Rouso, M. Sheves, X. Fu, S. Bressler, S. Druckmann, and M. Ottolenghi. 1997. Time-resolved titrations of Asp-85 in bacteriorhodopsin: the multicomponent kinetic mechanism. *Biochemistry.* 36:11369–11380.
- Frisch, M. J., G. W. Trucks, H. B. Schlegel, P. M. W. Gill, B. G. Johnson, M. A. Robb, J. R. Cheeseman, T. A. Keith, G. A. Petersson, J. A. Montgomery, K. Raghavachari, A. Al-Laham, V. G. Zakrzewski, J. V. Ortiz, J. B. Foresman, J. Cioslowski, B. B. Stefanov, A. Nanayakkara, M. Challacombe, C. Y. Peng, P. Y. Ayala, W. Chen, W. Wong, J. L. Andres, E. S. Replogle, R. Gomperts, R. L. Martin, D. J. Fox, J. S. Binkley, D. J. Defrees, J. Baker, J. J. P. Stewart, M. Head-Gordon, C. Gonzalez, and J. A. Pople. 1995. Gaussian 94, Pittsburgh PA.
- Fu, X., S. Bressler, M. Ottolenghi, T. Eliash, N. Friedman, and M. Sheves. 1997. Titration kinetics of Asp-85 in bacteriorhodopsin: exclusion of the retinal pocket as the color-controlling cation binding site. *FEBS Lett.* 416:167–170.
- Grigorieff, N., T. A. Ceska, K. H. Downing, J. M. Baldwin, and R. Henderson. 1996. Electron-crystallographic refinement of the structure of bacteriorhodopsin. *J. Mol. Biol.* 259:393–421.
- Henderson, R., J. M. Baldwin, T. A. Ceska, F. Zemlin, E. Beckmann, and K. H. Downing. 1990. Model for the structure of bacteriorhodopsin based on high-resolution electron cryo-microscopy. *J. Mol. Biol.* 213:899–929.
- Jonas, R., and T. G. Ebrey. 1991. Binding of a single divalent cation directly correlates with the blue-to-purple transition in bacteriorhodopsin. *Proc. Natl. Acad. Sci. USA.* 88:149–153.
- Kamikubo, H., M. Kataoka, G. Váró, T. Oka, F. Toyunaga, R. Needleman, and J. K. Lanyi. 1996. Structure of the N intermediate of bacteriorhodopsin revealed by x-ray diffraction. *Proc. Natl. Acad. Sci. USA.* 93:1386–1390.
- Kimura, Y., A. Ikegami, and W. Stoeckenius. 1984. Salt and pH-dependent changes of the purple membrane absorption spectrum. *Photochem. Photobiol.* 40:641–646.
- Kimura, Y., D. G. Vassilyev, A. Miyazawa, A. Kidera, M. Matsushima, K. Mitsuoka, K. Murata, T. Hirai, and Y. Fujiyoshi. 1997. Surface of bacteriorhodopsin revealed by high-resolution electron crystallography. *Nature.* 389:206–211.
- Kraulis, J. 1991. MOLSCRIPT: a program to produce both detailed and schematic plots of protein structure. *J. Appl. Cryst.* 24:946–950.
- Labarta, A., E. Molins, and J. Tejada. 1985. A new interpretation of the magnetic properties and electronic structure of manganese(II) phthalocyanine. *Z. Phys. B.* 58:299–304.
- Labarta, A., E. Molins, X. Viñas, J. Tejada, A. Caubet, and S. Alvarez. 1984. Electronic structure determination of iron(II) phthalocyanine via magnetic susceptibility and Mössbauer measurements. *J. Chem. Phys.* 80:444–448.
- Lanyi, J. K. 1993. Proton translocation mechanism and energetics in the light-driven pump bacteriorhodopsin. *Biochim. Biophys. Acta.* 1183:241–261.
- Logunov, I., W. Humphrey, K. Schulten, and M. Sheves. 1995. Molecular dynamics study of the 13-cis form (BR₅₄₈) of bacteriorhodopsin and its photocycle. *Biophys. J.* 68:1270–1282.
- Metz, G., F. Siebert, and M. Engelhard. 1992. Asp⁸⁵ is the only internal aspartic acid that gets protonated in the M intermediate and the purple-to-blue transition of bacteriorhodopsin. A solid-state ¹³C CP-MAS NMR investigation. *FEBS Lett.* 303:237–241.
- Miertus, S., E. Scrocco, and J. Tomasi. 1981. Electrostatic interaction of a solute with a continuum. A direct utilization of ab initio molecular potentials for the prevision of solvent effects. *Chem. Phys.* 55:117–124.
- Miertus, S., and J. Tomasi. 1982. Approximate evaluations of the electrostatic free energy and internal energy changes in solution processes. *Chem. Phys.* 65:239–245.
- Mowery, P. C., R. H. Lozier, L. Q. Chae, Y. Tseng, M. Tayler, and W. Stoeckenius. 1979. Effect of acid pH on the absorption spectra and photoreactions of bacteriorhodopsin. *Biochemistry.* 18:4100–4107.

- Oesterhelt, D., and W. Stoeckenius. 1971. Rhodopsin like protein from the purple membrane of *Halobacterium halobium*. *Nature New Biol.* 233: 149–152.
- Oesterhelt, D., and W. Stoeckenius. 1973. Functions of a new photoreceptor membrane. *Proc. Natl. Acad. Sci. USA.* 70:2853–2857.
- Oesterhelt, D., and W. Stoeckenius. 1974. Isolation of the cell membrane of *Halobacterium halobium* and its fractionation into red and purple membrane. *Methods Enzymol.* 31:667–678.
- Pebay-Peyroula, E., G. Rummel, J. P. Rosenbusch, and E. M. Landau. 1997. X-ray structure of bacteriorhodopsin at 2.5 angstroms from microcrystals grown in lipidic cubic phases. *Science.* 277:1676–1681.
- Roselli, C., A. Boussac, T. A. Mattioli, J. A. Griffiths, and M. A. El-Sayed. 1996. Detection of a Yb^{3+} binding site in regenerated bacteriorhodopsin that is coordinated with the protein and phospholipid head groups. *Proc. Natl. Acad. Sci. USA.* 93:14333–14337.
- Scharnagl, C., J. Hettenkofer, and S. F. Fischer. 1995. Electrostatic and conformational effects on the proton translocation steps in bacteriorhodopsin: analysis of multiple M structures. *J. Phys. Chem.* 99:7787–7800.
- Sepulcre, F., J. Cladera, J. García, M. G. Proietti, J. Torres, and E. Padrós. 1996. An EXAFS study of the high-affinity cation binding site in the purple membrane. *Biophys. J.* 70:852–856.
- Sepulcre, F., and E. Padrós. 1992. Fluorescence studies on the surface potential of deionized forms of purple and bleached membranes. In *Structures and Functions of Retinal Proteins*. J. L. Rigaud, editor. Colloque INSERM, John Libbey Eurotext Ltd. Montrouge. 225–228.
- Stuart, J. A., B. W. Vought, C.-F. Zhang, and R. R. Birge. 1995. The active site of bacteriorhodopsin. Two-photon spectroscopic evidence for a positively charged chromophore binding site mediated by calcium. *Bio-spectroscopy.* 1:9–28.
- Subramaniam, S., M. Gerstein, D. Oesterhelt, and R. Henderson. 1993. Electron diffraction analysis of structural changes in the photocycle of bacteriorhodopsin. *EMBO J.* 12:1–8.
- Subramaniam, S., T. Marti, and H. G. Khorana. 1990. Protonation state of Asp(Glu)-85 regulates the purple-to-blue transition in bacteriorhodopsin mutants Arg-82Ala and Asp-85Glu: the blue form is inactive in proton translocation. *Proc. Natl. Acad. Sci. USA.* 87:1013–1017.
- Tan, E. H. L., D. S. K. Govender, and R. R. Birge. 1996. Large organic cations can replace Mg^{2+} and Ca^{2+} ions in bacteriorhodopsin and maintain proton pumping ability. *J. Am. Chem. Soc.* 118:2752–2753.
- Thomanek, U. F., F. Parak, S. Formanek, and G. M. Kalvius. 1977. Mössbauer and susceptibility experiments on different compounds of Fe^{3+} -myoglobin. *Biophys. Struct. Mech.* 3:207–227.
- Zhang, Y. N., M. A. El-Sayed, M. L. Bonet, J. K. Lanyi, M. Chang, B. Ni, and R. Needleman. 1993. Effects of genetic replacements of charged and H-binding residues in the retinal pocket on Ca^{2+} binding to deionized bacteriorhodopsin. *Proc. Natl. Acad. Sci. USA.* 90:1445–1449.
- Zhang, Y. N., L. L. Sweetman, E. S. Awad, and M. A. El-Sayed. 1992. Nature of the individual Ca^{2+} binding sites in Ca^{2+} -regenerated bacteriorhodopsin. *Biophys. J.* 61:1201–1206.